

# QCD matter within a quasi-particle model and the critical end point

B. Kämpfer<sup>ab</sup>, M. Bluhm<sup>a\*</sup>, R. Schulze<sup>b</sup>, D. Seipt<sup>b</sup> and U. Heinz<sup>c</sup>

<sup>a</sup>Forschungszentrum Rossendorf, Institut für Kern- und Hadronenphysik,  
PF 510119, 01314 Dresden, Germany

<sup>b</sup>Technische Universität Dresden, Institut für Theoretische Physik,  
01062 Dresden, Germany

<sup>c</sup>Ohio State University, Department of Physics, Columbus, OH 43210, USA

We compare our quasi-particle model with recent lattice QCD results for the equation of state at finite temperature and baryo-chemical potential. The inclusion of the QCD critical end point into models is discussed. We propose a family of equations of state to be employed in hydrodynamical calculations of particle spectra at RHIC energies and compare with the differential azimuthal anisotropy of strange and charm hadrons.

## 1. QUASI-PARTICLE MODEL

The equation of state (EoS) of strongly interacting matter is a central issue to understand the hydrodynamical evolution in high-energy heavy-ion collisions. *Ab initio* evaluations based on QCD can deliver the EoS, e.g., in the form [1]

$$p = T^4 \left\{ c_0(T) + c_2(T) \left( \frac{\mu}{T} \right)^2 + c_4(T) \left( \frac{\mu}{T} \right)^4 + c_6(T) \left( \frac{\mu}{T} \right)^6 + \dots \right\}. \quad (1)$$

To arrive at a flexible parametrization of the EoS we have developed a quasi-particle model [2,3] using dynamically generated self-energies and a non-perturbative effective coupling as essential input. A comparison of the model with recent lattice data is exhibited in Fig. 1. The peak of  $c_4$  and the dipole shape of  $c_6$  emerge from a change of the effective coupling at the pseudo-critical temperature  $T_c(\mu_B = 0)$  dictated by the data. The calculation of the coefficients  $c_{2,4,6}$  requires the knowledge of the pressure  $p(T, \mu_B)$  at finite values of baryo-chemical potential  $\mu_B$  which is delivered by Peshier's equation [2]. The baryon number susceptibility follows directly from  $p(T, \mu_B)$ , see Fig. 1. The peak developing for  $\mu_B > 300$  MeV can be considered as a signal of some critical behavior.

## 2. CRITICAL END POINT

QCD for finite quark masses displays a critical end point (CEP) [4] where a phase transition of first order sets in at finite values of  $\mu_B$ . The CEP belongs to the universality class of the 3D Ising model characterized by a set of critical exponents. A convenient

---

\*Supported by BMBF and GSI-FE.

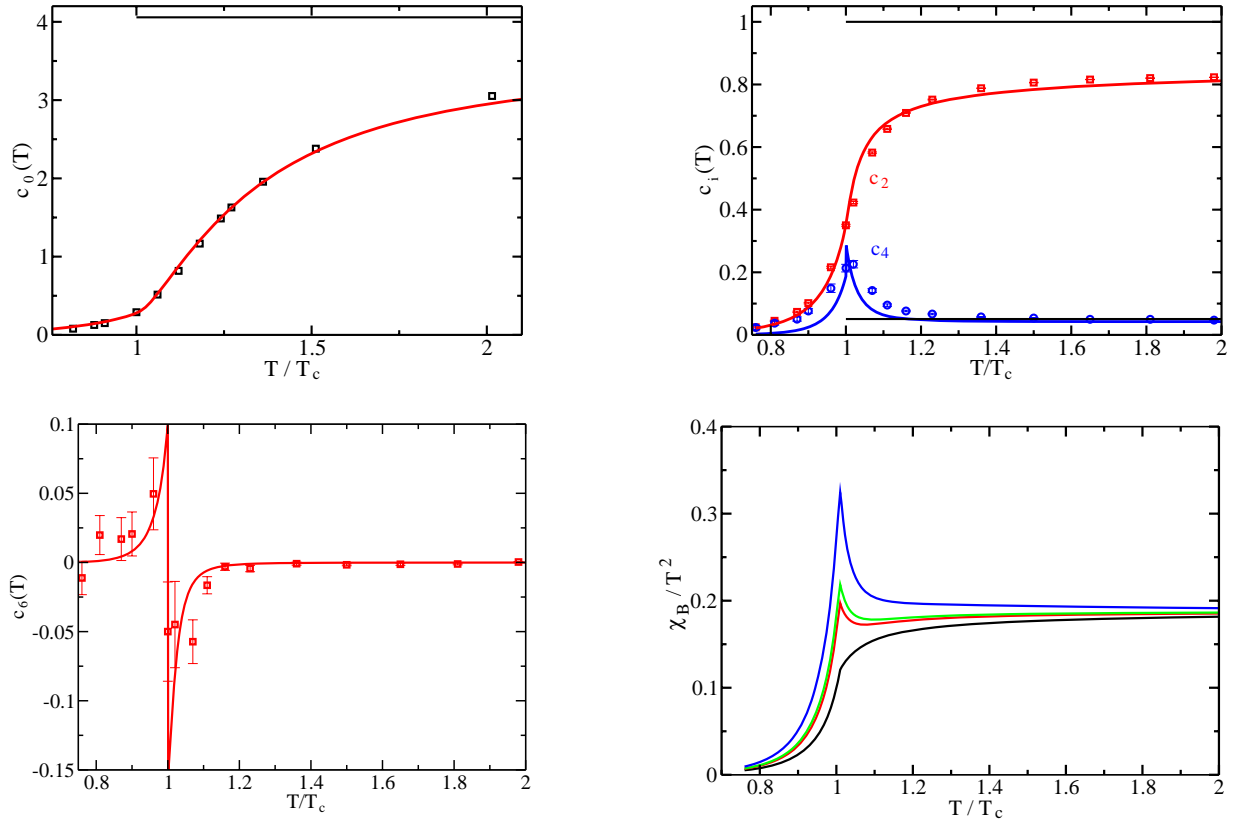


Figure 1. The Taylor expansion coefficients  $c_{0,2,4}$  (top row, horizontal lines depict the corresponding terms in the bag model) and  $c_6$  (left panel in bottom row) of the equation of state as a function of the scaled temperature. QCD lattice data from [1,5]. Right panel in bottom row: baryon number susceptibility ( $\mu_B = 450, 330, 300, 150$  MeV from top to bottom). For details see [3].

parametric representation of the singular part (formulated in terms of the entropy density  $s$ ) of the EoS can be found in [6]. The complete EoS is accordingly

$$s = s_{reg} + s_{sing}. \quad (2)$$

While the location of the CEP is determined by lattice QCD calculations [7] the size of the critical region is barely known. A simple toy model demonstrating the effect of  $s_{sing}$  for given  $s_{reg}$  is  $s_{reg} = 4\bar{c}_0 T^3 + 2\bar{c}_2 \mu_B^2 T$  and  $s_{sing} = s_{reg} A \tanh \mathcal{S}_c$  with the same  $\mathcal{S}_c$  as in [8] and  $\bar{c}_0 = (32 + 21N_f)\pi^2/180$  and  $\bar{c}_2 = N_f/18$  for  $N_f = 2$ . We assume a critical line given by  $T(\mu_B) = T_c(1 - c(\mu_B/T_c)^2)$  with  $c = 0.0077$  from [9] and locate the CEP at  $\mu_B = 330$  MeV according to [7]. This information is needed to map the coordinates of  $s_{sing}$  into the  $T - \mu_B$  plane. A typical pattern of isentropic trajectories is exhibited in Fig. 2. The pattern (left panel) seems to be generic (see also [8] for another model with CEP): trajectories which are left [right] to the CEP for small values of the strength parameter  $A$  are attracted [repelled], but at variance to lattice QCD results (right panel).

The proper implementation of CEP phenomena in our quasi-particle model is under consideration.

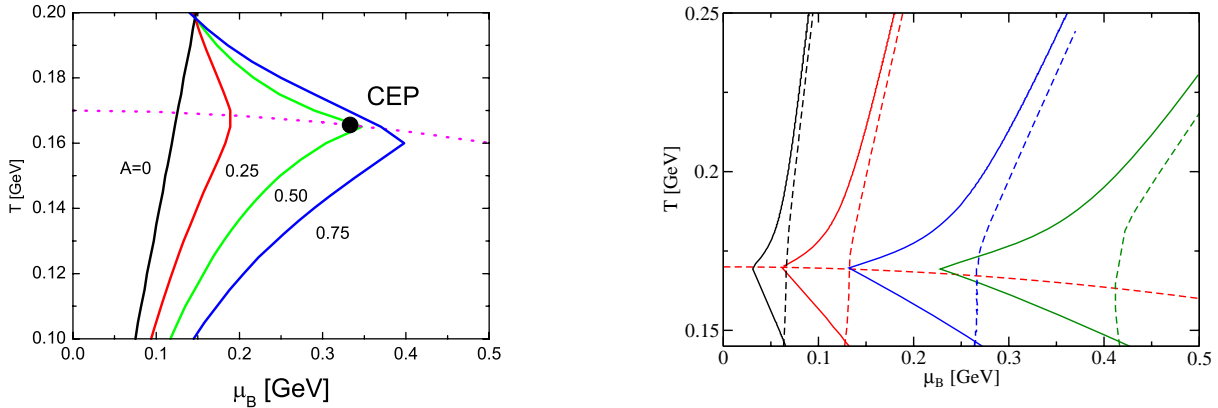


Figure 2. Isentropic trajectories and the (pseudo-)critical line in the  $T - \mu_B$  plane. Left panel: a toy model including the CEP (entropy per baryon = 100, various strength parameters  $A$  as indicated). Right panel: quasi-particle model adjusted to lattice QCD data [1,5] via  $c_0$  (solid curves) or  $c_2$  (dashed curves); both fits agree within 10% for  $p(T, \mu_B = 0)$ ; entropy per baryon = 200, 100, 50, 33, from left to right.

### 3. A FAMILY OF EQUATIONS OF STATE, HYDRODYNAMICS AND AZIMUTHAL ANISOTROPY

It is expected that lattice QCD data at high temperature are realistic, as improved actions have been used. At low temperature, the employed quark masses are too large to give realistic results. These however agree with the resonance gas model once analog assumptions are implemented [10]. It is therefore reasonable to use the resonance gas model at low  $T$  and employ our quasi-particle model to extrapolate lattice QCD results both to larger  $\mu_B$  and smaller  $T$  as long as a systematic chiral extrapolation can not be done safely due to lacking lattice QCD input.

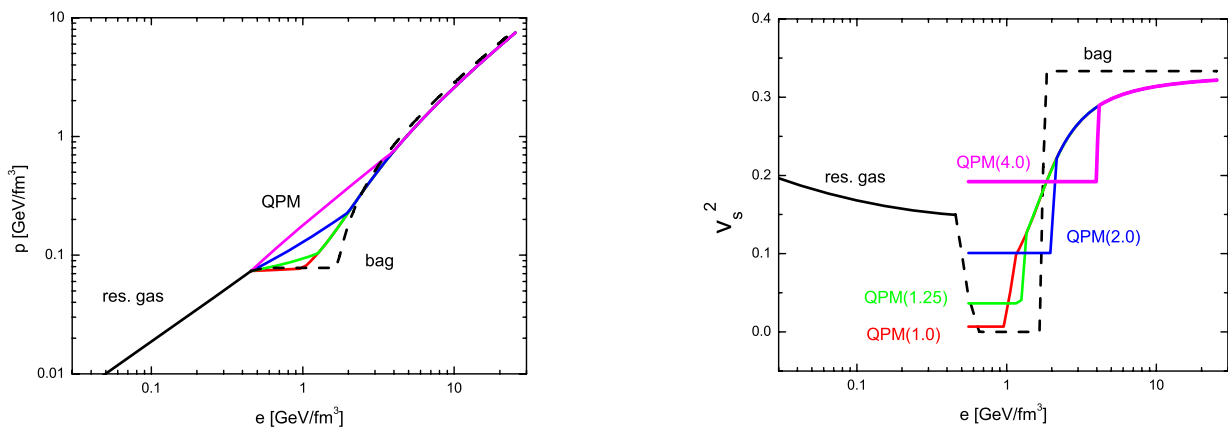


Figure 3. A family of EoS's by combining our quasi-particle model and the resonance gas model for baryon densities relevant for top RHIC energies: pressure (left, QPM(4.0), QPM(2.0), QPM(1.25), QPM(1.0), from top to bottom) and squared sound velocity (right) as a function of energy density. Bag model results are depicted by dashed curves.

We generate a family of EoS's by keeping the matching point to the resonance gas EoS fixed and interpolate linearly to a given matching point (given by energy density which serves as label) of the quasi-particle model. Such a family is exhibited in Fig. 3. Surprising is the similarity of QPM(1.0) and the bag model EoS used in [11]. Equipped with such a QCD based EoS one can compare results of hydrodynamical calculations with data, e.g., for the azimuthal anisotropy  $v_2$ . Examples are exhibited in Fig. 4 for  $\Lambda$ ,  $\Xi$ ,  $\Omega$ ,  $\phi$ ,  $D$ .

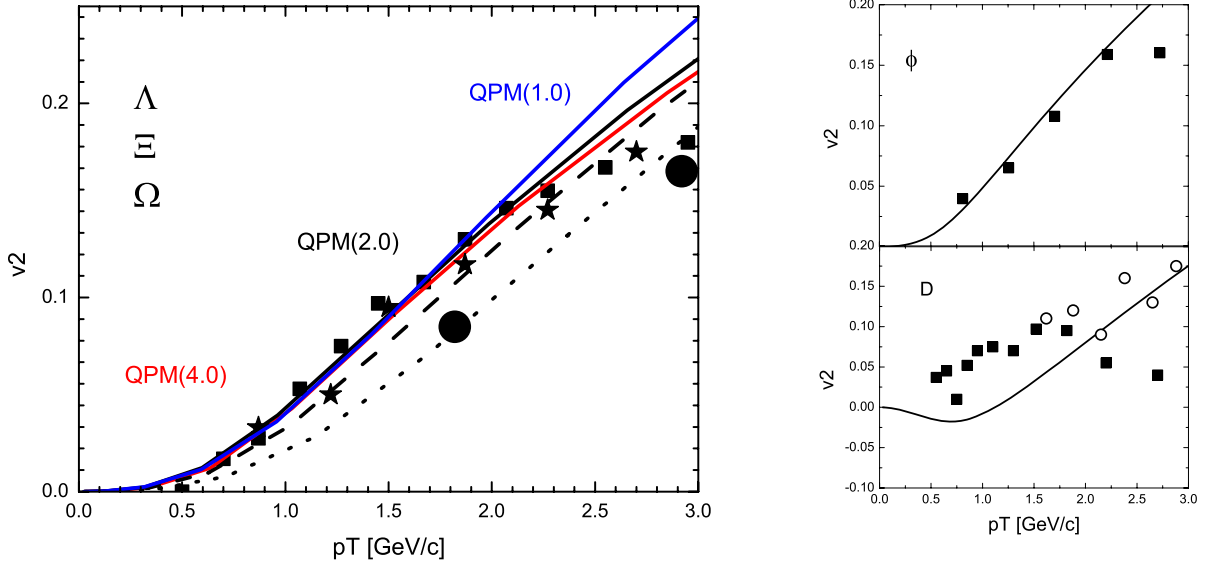


Figure 4.  $v_2$  as a function of transverse momentum. Left: strange baryons (solid curves QPM(1.0), QPM(2.0), QPM(4.0) [from top to bottom, with decoupling temperatures adjusted to data up to 2.5 GeV/c] and squares:  $\Lambda$ , dashed curve [QPM(2.0)] and stars:  $\Xi$ , dotted curve [QPM(2.0)] and circles:  $\Omega$ , data from [12]), right top:  $\phi$  (data from [13]), right bottom:  $D$  (data from [14]), both for QPM(2.0). Impact parameter  $b = 5.2$  fm.

## REFERENCES

1. C.R. Allton et al., Phys. Rev. D 68 (2003) 014507, Phys. Rev. D 71 (2005) 054508
2. A. Peshier et al., Phys. Rev. D 54 (1996) 2399 (1996), Phys. Rev. C 61 (2000) 045203, Phys. Rev. D 66 (2002) 094003
3. M. Bluhm, B. Kämpfer, G. Soff, Phys. Lett. B 620 (2005) 131
4. Z. Fodor, S.D. Katz, JHEP 0203 (2002) 014 and references therein
5. F. Karsch, E. Laermann, A. Peikert, Phys. Lett. B 478 (2000) 447
6. R. Guida, J. Zinn-Justin, Nucl. Phys. B 489 (1997) 626
7. Z. Fodor, S.D. Katz, JHEP 0404 (2004) 050
8. C. Nonaka, M. Asakawa, Phys. Rev. C 71 (2005) 044904
9. C.R. Allton et al., Phys. Rev. D 66 (2002) 074507
10. F. Karsch, K. Redlich, A. Tawfik, Phys. Lett. B 571 (2003) 67
11. P.F. Kolb, U. Heinz, Quark Gluon Plasma, (Eds.) R. Hwa, X.N. Wang, p. 634
12. J. Adams et al. (STAR), nucl-ex/0504022
13. M. Oldenburg (STAR), talk at QM2005
14. Y. Akiba (PHENIX), talk at QM2005; F. Laue et al. (STAR), nucl-ex/0411007